KTeV Determination of the CKM Parameter $|V_{us}|$

R. Kessler (for the KTeV collaboration) [a]

[a]Enrico Fermi Institute, University of Chicago, Illinois 60637

KTeV has recently reported results for the six largest K_L branching fractions, and also for the form factors in $K_L \to \pi^\pm e^\mp \nu$ and $K_L \to \pi^\pm \mu^\mp \nu$ decays. Using these results, we present a new determination of the CKM parameter $|V_{us}|$.

1. Introduction

For more than two decades, the first row of the Cabibbo-Kobayashi-Maskawa (CKM) matrix has suggested a two-sigma discrepancy in the unitarity condition. The first hint of resolving this discrepancy came last year when Brookhaven Experiment E865 reported that their measurement of $B(K^+ \to \pi^0 e^+ \nu)$ [1] is 6% higher than the PDG average [2]; the resulting $|V_{us}|$ value is consistent with unitarity. To address the situation in which $|V_{us}|$ is extracted from K_L decays, KTeV has recently measured the K_L semileptonic branching fractions [3] and form factors [4]. An overview of the $|V_{us}|$ extraction from our results has been reported in [5]. In this paper, we give a brief description of the technique and results.

The $K_L \to \pi^\pm \ell^\mp \nu$ ($K_{\ell 3}$) decay rate is related to $|V_{us}|$ by

$$\Gamma_{K\ell 3} = \frac{G_F^2 M_K^5}{192\pi^3} S_{EW}(1+\delta_K^\ell)\,|V_{us}|^2\, f_+^2(0) I_K^\ell, \quad (1)$$

where ℓ refers to either e or μ, G_F is the Fermi constant, M_K is the kaon mass, S_{EW} is the short-distance radiative correction, δ_K^ℓ is the mode-dependent long-distance radiative correction, $f_+(0)$ is the calculated form factor at zero momentum transfer for the $\ell\nu$ system, and I_K^ℓ is the phase-space integral, which depends on measured semileptonic form factors. The experimental input includes the semileptonic branching fractions, form factors, and K_L lifetime; the theoretical input includes radiative corrections and $f_+(0)$.

To improve the $|V_{us}|$ determination with K_L decays, the KTeV experiment at Fermilab has measured the six largest K_L branching fractions, which account for more than 99.9% of the decay rate, and we have also measured the semileptonic form factors to determine I_K^e and I_K^μ. In our $|V_{us}|$ determination, the K_L lifetime is the only experimental input that we take from the PDG. Previous $|V_{us}|$ determinations from both neutral and charged kaons are based on K_{e3} decays; $K_{\mu 3}$ decays have not been used (by PDG) because the $K_{\mu 3}$ form factor, and hence I_K^μ, was poorly determined. Here we determine $|V_{us}|$ from both K_{e3} and $K_{\mu 3}$ with comparable precision, and the consistency of these two $|V_{us}|$ determinations (Sec. 2.3) is an important crosscheck. The KTeV measurements are based on high statistics samples (10^5–10^6), and we take advantage of the precise calibrations and Monte Carlo simulation used in our ϵ'/ϵ analysis.

2. KTeV Measurements

The KTeV detector, analysis, and Monte Carlo simulation [MC] of the K_L decay modes are described elsewhere [3,4]. The overall quality of the simulation is shown by the agreement in the data and MC decay vertex distributions (Fig. 1); the kaon energy distributions [3] also agree well. A significant improvement in the $|V_{us}|$ analysis is a new treatment of radiative effects in the MC generator for semileptonic decay modes. The program KLOR [6] is used to generate $K_L \to \pi^\pm \ell^\mp \nu(\gamma)$; KLOR includes virtual photon exchange between the charged particles, and inner Bremsstrahlung (IB) off the pion, lepton and

decay vertex. The effects of IB are most important in the K_{e3} decay mode in which IB modifies the acceptance by $\sim 3\%$. Radiative effects are also important in the form factor measurements (Sec. 2.2).

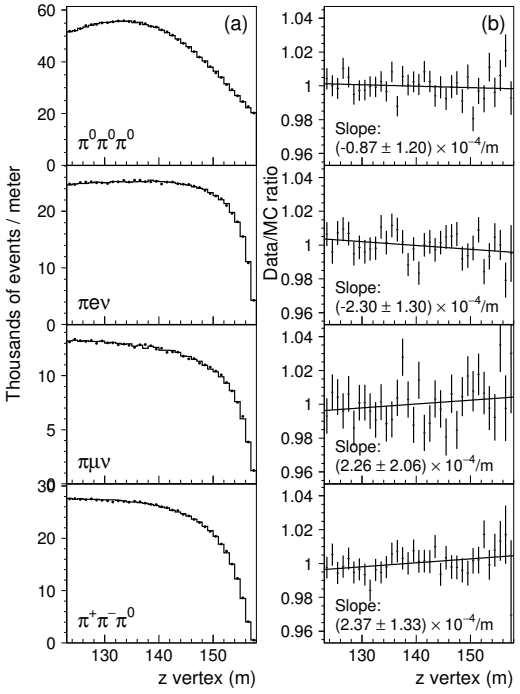

Figure 1. Reconstructed decay vertex for the four main K_L decay modes, for data (dots) and MC (histogram). The data/MC ratio, along with a linear fit, are shown on the right of each distribution; the slope of the fit is indicated on the plot.

2.1. K_L Branching Fractions

To determine the K_L branching fractions, we have measured the following five partial-width ratios:

$$\Gamma_{K\mu 3}/\Gamma_{Ke3} \equiv \Gamma(K_L \to \pi^\pm\mu^\mp\nu)/\Gamma(K_{e3}) \quad (2)$$

$$\Gamma_{+-0}/\Gamma_{Ke3} \equiv \Gamma(K_L \to \pi^+\pi^-\pi^0)/\Gamma(K_{e3}) \quad (3)$$

$$\Gamma_{000}/\Gamma_{Ke3} \equiv \Gamma(K_L \to \pi^0\pi^0\pi^0)/\Gamma(K_{e3}) \quad (4)$$

$$\Gamma_{+-}/\Gamma_{Ke3} \equiv \Gamma(K_L \to \pi^+\pi^-)/\Gamma(K_{e3}) \quad (5)$$

$$\Gamma_{00}/\Gamma_{000} \equiv \Gamma(K_L \to 2\pi^0)/\Gamma(K_L \to 3\pi^0) \quad (6)$$

where $\Gamma(K_{e3}) \equiv \Gamma(K_L \to \pi^\pm e^\mp\nu)$. Each ratio uses a statistically independent sample, and each pair of decay modes is recorded in the same trigger to avoid uncertainties in the trigger efficiency.

The partial-width ratio results are given in [3, 5]. The largest uncertainty is 1.2% on $\Gamma_{000}/\Gamma_{Ke3}$ because this ratio does not benefit from detector efficiency cancellations; the uncertainties on the other partial-width ratios are between 0.4% and 0.6%. The ratios with Γ_{Ke3} in the denominator show significant disagreement compared with the PDG value [2]; only Γ_{00}/Γ_{000} is consistent with PDG. Each partial-width ratio is measured using high- and low-intensity data samples, in which there is a factor of ten difference in beam intensity between the two samples. As shown in Fig. 2, results from the two samples agree well. The measurement with the smaller uncertainty is used for the final result.

Assuming that these six branching fractions sum to 0.9993[1], the partial-width ratios are converted into branching fractions; the KTeV and PDG-fit branching fractions are plotted in Fig. 3. The KTeV/PDG ratio for the six branching fractions are shown in Fig. 4. Four of the six branching fractions show a large deviation from PDG fit value; only $B(K_L \to \pi^\pm\mu^\mp\nu)$ and $B(K_L \to \pi^+\pi^-\pi^0)$ are consistent with PDG.

2.2. Semileptonic Form Factors

To determine the phase space integrals, I_K^e and I_K^μ, we have measured the semileptonic form factors with the following parametrization:

$$f_+(t) = f_+(0)\left[1 + \lambda'_+\frac{t}{m_\pi^2} + \frac{1}{2}\lambda''_+\frac{t^2}{m_\pi^4}\right], \quad (7)$$

$$f_0(t) = f_+(0)\left[1 + \lambda_0\frac{t}{m_\pi^2}\right], \quad (8)$$

where m_π is the mass of the charged pion and t is the square of the four-momentum transfer to the lepton-neutrino system. Ignoring the effects of radiation, $t = (P_K - p_\pi)^2 = (p_\ell + p_\nu)^2$. Since the neutrino is undetected, there are two kaon energy solutions resulting in two solutions for t. To avoid this twofold ambiguity in t, we

[1]The missing K_L decay channels (from PDG) are $B(K_L \to \gamma\gamma) = 0.060\%$, $B(K_L \to \pi^0\pi^\pm e^\mp\nu) = 0.005\%$, and the direct emission $B(K_L \to \pi^+\pi^-\gamma) = 0.002\%$

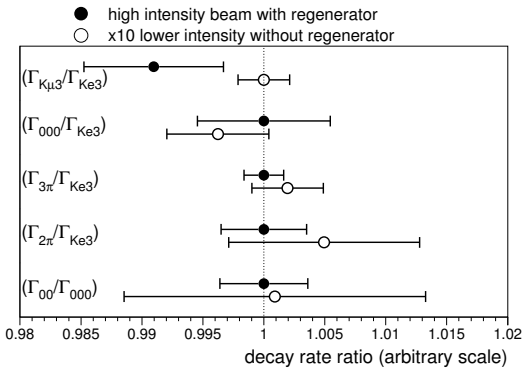

Figure 2. Comparison of partial-width ratios measured using high and low intensity data samples. The scale is chosen so that the nominal KTeV result is 1. The errors reflect statistical uncertainties.

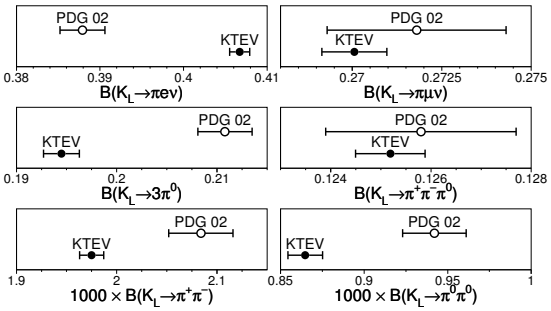

Figure 3. The six largest K_L branching fractions measured by KTeV (solid dots) and from PDG 02 (open circles).

define "$t_\perp$" quantities using momentum components transverse to the kaon flight direction: $t_\perp^\pi$ is based on the transverse components of P_K and p_π, where the transverse component of the kaon momentum is zero by definition, and $t_\perp^\ell$ is based on the transverse components of p_ℓ and p_ν. Precise definitions of $t_\perp^\pi$ and $t_\perp^\ell$ are given in [4]. The important features of these variables are

- both $t_\perp$ variables are strongly correlated with t; compared to an ideal t-based analysis, the loss in statistical precision is $\sim 15\%$.
- For K_{e3}, $t_\perp^\pi$ is much less sensitive to radiative effects compared to $t_\perp^\ell$.
- Since both $t_\perp$ variables are invariant under kaon boosts, these distributions are insensitive to the kaon energy spectrum.
- $t_\perp$ is uniquely determined for each event.

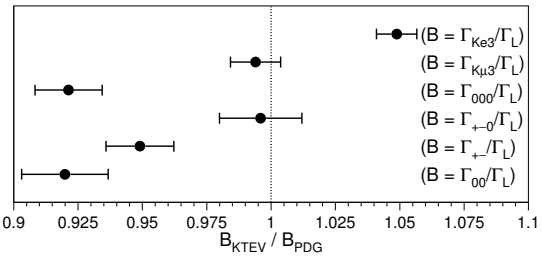

Figure 4. The KTeV/PDG02 ratio for the six branching fractions shown in Fig. 3.

The analysis consists of determining the form factor values that result in the best data-MC agreement in the $t_\perp$ distributions. Compared to PDG, $f_+(t)$ is measured with three times better precision, and $f_0(t)$ is measured with five times better precision. For $f_+(t)$, the contours of λ''_+ vs. λ'_+ are shown in Fig. 5. This plot shows the first evidence (4σ) of the second-order term (λ''_+) in K_L decays.[2] The significance of our λ''_+ measurement is illustrated in Fig. 6, which compares the $t_\perp^\pi$ data distribution to MC. Using a linear model for $f_+(t)$, and then generating MC based on the best fit λ_+, there is a clear data-MC discrepancy; for the nonlinear model, however, the data and MC $t_\perp^\pi$ distributions show good agreement.

Figure 7 shows some crosschecks for the K_{e3} analysis using a linear model; *i.e*, fitting only for λ_+. The first crosscheck shows consistent results using either the $t_\perp^\pi$ or $t_\perp^e$ variable. The results with "Born MC" ignore radiative effects. Using the $t_\perp^\pi$ variable, radiative effects have a small effect; using the $t_\perp^e$ variable, radiative effects are much more significant. The effect of a 50 μm shift

[2] In $K^- \to \pi^0 e^- \nu$ decays, ISTRA+ has recently reported a second-order term with 2σ significance.[7].

in the drift chamber position[3] is clearly visible when the form factor is determined for different magnet polarities and lepton charges. Finally, λ_+ is consistent using different neutrino angle ranges. Note that $\cos(\theta_\nu) < 0.4$ corresponds to kaon energy solutions that differ by 18% on average, and $\cos(\theta_\nu) > 0.4$ corresponds to a 40% difference.

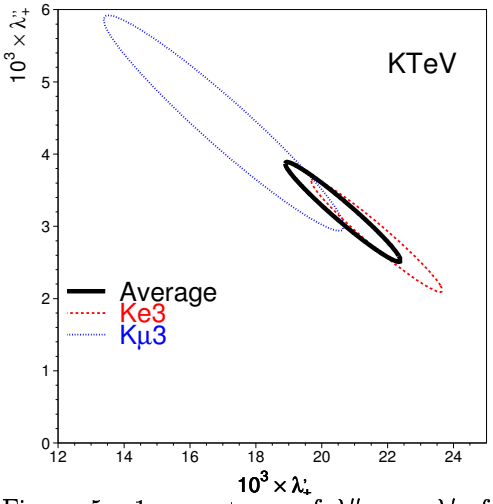

Figure 5. 1 σ contours of λ''_+ vs. λ'_+ for K_{e3} (dashed), $K_{\mu 3}$ (dotted), and the average of both decay modes (solid curve).

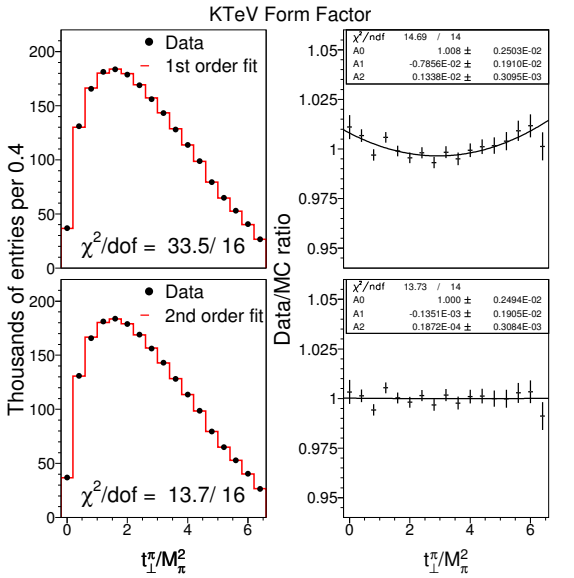

Figure 6. Data and MC distributions for $t^\pi_\perp$ in K_{e3} decays (left) and data/MC ratios (right). The data (dots) are the same in both the upper and lower plots. For MC (histogram), the upper plot is based on a linear model fit (λ_+ only), and the lower plot uses the nominal second-order fit (λ'_+ and λ''_+).

Although the KTeV form factors have much improved precision, leading to 0.3% statistical uncertainty in the I^ℓ_K integrals, the model dependence in the form factor parametrization limits the systematic precision on I^ℓ_K. Specifically, we find that a pole model gives a good fit to our data, but results in a 0.7% shift in the I^ℓ_K integrals compared to the nominal parametrization in Eqs. 7-8. This 0.7% shift is included as a systematic uncertainty in our extraction of $|V_{us}|$.

The quality of the Monte Carlo simulation and the KLOR generator is shown by a data-MC comparison of the reconstructed pion-lepton invariant mass, $m_{\pi\ell}$. In Fig. 8, data and MC show excellent agreement in the $m_{\pi\ell}$ distributions, with $\chi^2/dof = 35/32$ for K_{e3} and 23/25 for $K_{\mu 3}$. To illustrate our sensitivity to the precise modeling of radiative corrections, consider a test case in which we use the approximate radiative generator PHOTOS [8] (instead of KLOR), and repeat the form factor analysis. In this test scenario, λ_+ increases by $2\sigma_{\rm stat}$ and λ_0 increases by $8\sigma_{\rm stat}$; however, the corresponding χ^2/dof in the $m_{\pi\ell}$ distributions increases to 57/32 and 39/25 for K_{e3} and $K_{\mu 3}$, respectively, showing the limitation of radiative corrections from PHOTOS. This exercise with PHOTOS illustrates that an accurate treatment of radiative corrections is necessary to extract precise form factors, and that an approximate treatment of radiative effects would result in data-MC discrepancies in kinematic distributions such as the pion-lepton mass and transverse momentum.

[3]Systematic errors are based on 20 μm uncertainty in the drift chamber alignment.

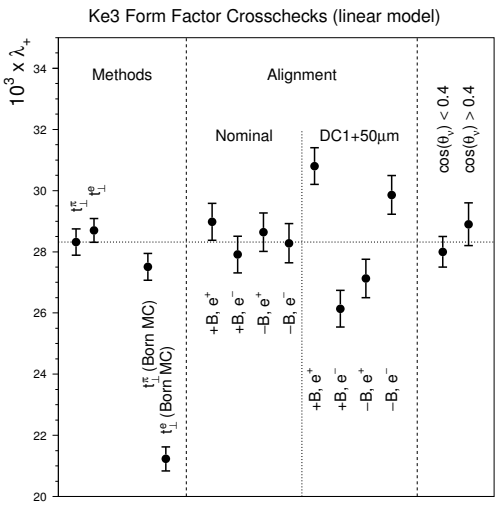

Figure 7. Crosschecks on the λ_+ form factor obtained from K_{e3} decays using a linear model (*i.e*, ignoring λ_+'' in Eq. 7). The horizontal dotted line shows the nominal result based on $t_\perp^\pi$. "Born MC" refers to results based on MC simulations using only Born-level matrix element and ignoring radiative effects. Under "alignment," $\pm B$ refers to the polarity of the analysis magnet, and $e^\pm$ refers to the electron and positron. θ_ν is the neutrino angle relative to the kaon flight direction (in kaon center-of-mass frame).

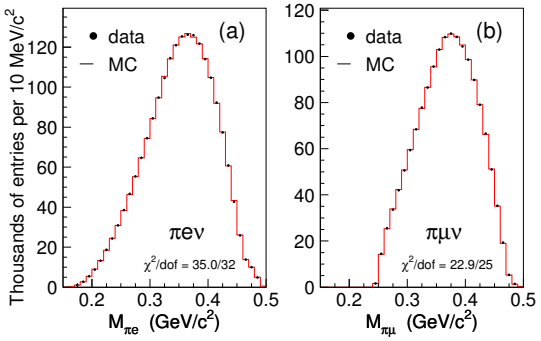

Figure 8. In the KTeV form factor analysis, distribution of (a) pion-electron mass for $K_L \to \pi^\pm e^\mp \nu$, and (b) pion-muon mass for $K_L \to \pi^\pm \mu^\mp \nu$. Data are shown as dots; MC as histogram.

2.3. Summary of Changes

Here is a summary of changes in the experimental input that is used to extract $|V_{us}|$ from Eq. 1:

- KTeV $B(K_{e3})$ is 5% higher compared to PDG (Fig. 3).
- KTeV $B(K_{\mu 3})$ is consistent with PDG.
- KTeV I_K^e is 1.7% lower than PDG.
- KTeV I_K^μ is 4.2% lower than PDG.

Note that both I_K^ℓ integrals include a -1% shift due to the second-order term in the form factor (λ_+'' in Eq. 7). The impact of these measurements will clearly increase $|V_{us}|$ by a few percent. A new feature in this analysis is that we also use $K_{\mu 3}$ to determine $|V_{us}|$ because λ_0 is sufficiently well measured such that both I_K^e and I_K^μ have comparable precision.

An important test of the new KTeV results compares G_F for the two decay modes by taking the ratio of Eq. 1 for $K_L \to \pi^\pm \mu^\mp \nu$ and $K_L \to \pi^\pm e^\mp \nu$:

$$\left(\frac{G_F^\mu}{G_F^e}\right)^2 = \left[\frac{\Gamma(K_L \to \pi^\pm \mu^\mp \nu)}{\Gamma(K_L \to \pi^\pm e^\mp \nu)}\right] \Big/ \left(\frac{1+\delta_K^\mu}{1+\delta_K^e} \cdot \frac{I_K^\mu}{I_K^e}\right). \quad (9)$$

The ratio of radiative corrections is calculated to be $(1+\delta_K^\mu)/(1+\delta_K^e) = 1.0058 \pm 0.0010$ [6], the ratio of the phase space integrals is $I_K^\mu/I_K^e = 0.6622 \pm 0.0018$ [4], and $\Gamma_{K\mu 3}/\Gamma_{Ke3} = 0.6640 \pm 0.0026$ [3]. The resulting ratio of couplings squared is $(G_F^\mu/G_F^e)^2 = 0.9969 \pm 0.0048$, consistent with lepton universality. The same ratio calculated from PDG widths and form factors is $(G_F^\mu/G_F^e)^2 = 1.0270 \pm 0.0182$. Note that the 0.5% uncertainty in our universality test is much smaller than the differences between the KTeV and PDG partial-width ratios and phase space integrals.

3. Determination of $|V_{us}|$

The theoretical inputs to Eq. 1 are:

- $S_{EW} = 1.022$ from [9] (cutoff at the proton

mass)

- $\delta_K^e = 0.013(3)$ and $\delta_K^\mu = 0.019(3)$ from [6]
- $f_+(0) = 0.961 \pm 0.008$ from [10].

As described in [5], we average the $|V_{us}|$ values from $K_L \to \pi^\pm e^\mp \nu$ and $K_L \to \pi^\pm \mu^\mp \nu$ decays and find

$$|V_{us}| f_+(0) = 0.2165 \pm 0.0012 \quad (10)$$

$$|V_{us}| = 0.2252 \pm 0.0008_{\rm KTeV} \pm 0.0021_{\rm ext} \quad (11)$$

where the external error is from $f_+(0)$, τ_L, and radiative corrections. Using $|V_{ud}|$ and $|V_{ub}|$ from PDG [2], and $|V_{us}|$ from Eq. 11,

$$1 - |V_{ud}|^2 - |V_{us}|^2 - |V_{ub}|^2 = 0.0018 \pm 0.0019 \,, \quad (12)$$

consistent with unitarity.

3.1. Comparison with Other Measurements and with Theory

A comparison of $|V_{us}| f_+(0)$ determinations is shown in Fig. 9. Note that the uncertainty in the experimental quantity $|V_{us}| f_+(0)$ (circles) does not include the $\sim$ 1% theoretical uncertainty from $f_+(0)$, but does include the 0.4% uncertainty from the external measurement of the kaon lifetime, and the 0.15% uncertainty from radiative corrections. $|V_{us}| f_+(0)$ based on the KTeV K_L measurements is 3% (5σ!) higher than PDG. There is a similar discrepancy between E865 and PDG in the K^+ sector. However, the KTeV result cannot distinguish between these two evaluations based on K^+ decays. The corresponding prediction based on unitarity, $f_+(0)\sqrt{1 - |V_{ud}|^2 - |V_{ub}|^2}$ (open squares in Fig 9), includes uncertainties from both $f_+(0)$ and $|V_{ud}|$.

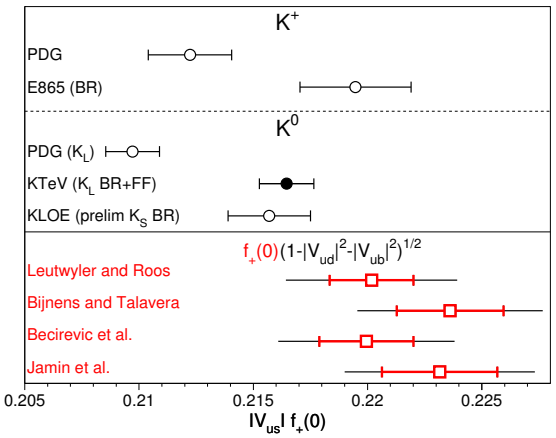

Figure 9. Comparison of $|V_{us}| f_+(0)$ determined with K^+ and K^0 decays. The solid dot is based on the KTeV branching fractions and form factors [5]. The E865 result is from [1], and the preliminary result from KLOE is based on K_S decays [11]. The PDG values are evaluated by KTeV using the PDG branching fractions, lifetimes, and form factors. The open squares show different theoretical values of $f_+(0)$[10,12–14] multiplied by $\sqrt{1 - |V_{ud}|^2 - |V_{ub}|^2}$; the inner error bar shows the theory uncertainty on $f_+(0)$ and the total error includes the uncertainty on $|V_{ud}|$.

REFERENCES

1. A. Sher *et al.;* (BNL E865), Phys. Rev. Lett. **91**, 261802 (2003)
2. Particle Data Group, Phys. Rev. D **66**, 1 (2002)
3. T. Alexopoulis *et al.;* (KTeV), submitted to Phys. Rev. D, hep-ex/0406002.
4. T. Alexopoulis *et al.;* (KTeV), submitted to Phys. Rev. D, hep-ex/0406003.
5. T. Alexopoulis *et al.;* (KTeV), submitted to Phys. Rev. Lett, hep-ex/0406001.
6. T. Andre, hep-ph/0406006. Also see talk by T. Andre in these proceedings.
7. O.P. Yushchenko *et al.;* (ISTRA+), Phys. Lett. B **589**, 111 (2004)
8. E. Barberio and Z.Was, Comput. Phys. Commun. **79**, 291 (1994)
9. W. Marciano and A. Sirlin, Phys. Rev. Lett. bf 56, 22 (1986)
10. H .Leutwyler and M. Roos, Z. Phys. C **25**, 91 (1984)
11. See talk by A. Antonelli at HQL 2004.
12. J. Bijnens and P. Talvera, Nucl. Phys. B **669**, 341 (2003)
13. D. Becirevic *et al.;*, hep-ph **0403217** (2004)
14. M. Jamin *et al*, JHEP **02**, 047 (2004)